Numerical Investigation of RANS based CFD with STAR-CCM+ Code Using Sodium-Cooled Experimental Thermal Data

Han-Seop Song[a], Jonggan Hong[b], Yo-Han Jung[b], Jae-Ho Jeong[a*]
[a]*Gachon University, 1342, Seongnam-daero, Sujeong-gu, Seongnam-si, Gyeonggi-do*
[b]*Korea Atomic Energy Research Institute, 111 Daedeok-daero, 989 Beon-gil, Yuseong-gu,, DaeJeon 34057*
[*]*Corresponding author: jaeho.jeong@gachon.ac.kr*

1. Introduction

The Gen-IV SFR (Sodium-cooled Fast Reactor) is a reactor that uses fast neutrons to cause fission reactions and uses sodium as a coolant to transfer heat. SFR is receiving a lot of attention from many countries as a future nuclear energy because it uses liquid metal to make it compact, high power density, and highly stability. It is important to accurately predict the speed and temperature profile of the coolant in the fuel assembly. High heat generated by fission can cause thermal stress in the clad when a large temperature change occurs around the fuel tube. In addition, determining the highest cladding temperature, hotspot location and temperature gradient in hexagonal ducts is important for design and safety analysis decisions.

In this study, the Reynolds-averaged Navier-Stokes equation (RANS) based CFD Methodology was validated based on an existing sodium cooled experimental data. For the experimental data, ORNL19 pin and Toshiba 37 Pin, whose geometric conditions for CFD analysis have been published, were used. The thermal hydraulic behavior of fuel assemblies was compared using the computational fluid dynamics codes STAR-CCM+. The RANS based CFD methodology is implemented with high resolution scheme in convection term and Shear Stress Transport (SST) turbulence model for the ORNL 19 pin and Toshiba 37 pin wire-wrapped fuel assembly. [1,2]

2. NUMERICAL METHOD

2.1 Computational grid system

Fig. 1 shows the computational grid configuration of the fuel assembly. An innovative grid generation method using Fortran-based in-house code was applied. [3] Since heat transfer also occurs due to thermal conduction of the wire and the cladding, two interfaces were added by additionally creating a grid of rods and wires to simulate the same as in the experiment. Because the actual wire shape is simulated without distortion of the shape, the prediction of the contact area between the wire and the rod can be made more accurately. Simulation results using this methodology have been proven that it is possible to accurately predict the pressure drop and flow analysis of the fuel assembly [4].

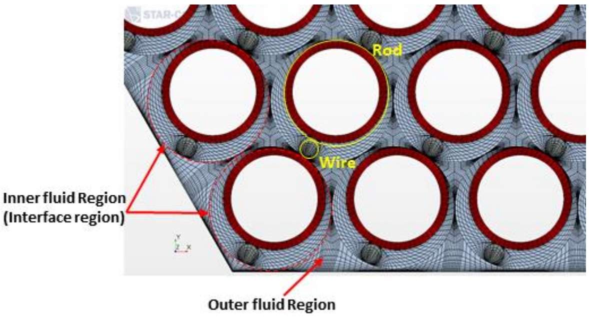

Fig 1. Computational grid system of the fuel assembly

2.2 CFD analysis Method

CFD analysis was performed based on ORNL 19 pin and Toshiba 37 pin experimental data [1,2]. The main design variables are shown in Table I. The experimental conditions used for the CFD analysis are shown in Table II. The inlet is defined as a mass flow rate of various values and the outlet is defined as a constant outlet pressure of 0 Pa. The surface of the rods and wire spacers is defined with a no-slip condition with a smooth roughness. The duct wall is also applied under a no-slip condition with a smooth roughness.

Table I. Geometric information of fuel assembly

	ORNL 19 pin	Toshiba 37 pin
Geometry Parameters	Values	
Number of pins	19	37
Pin diameter	5.84 mm	6.5 mm
Wire diameter	1.40 mm	1.32 mm
Wire lead pitch	304.8 mm	307 mm
Pin pitch	7.26 mm	7.87 mm
Heated length	533.4 mm	923.8 mm
Total length	914.4 mm	1328 mm

Table II. Experimental conditions used for CFD

	Test No.	Inlet Temp [°C]	Flow rate [kg/s]	Power [kW]	Skew [Max/ Min]
ORNL 19 pin	Test 2	315.55	2.932	166.25	1:1
	Test 3	315.55	2.932	166.25	1.2:1
	Test 14	315.55	2.932	166.25	3:1
Toshiba 37pin	C37P06	203.5	0.374	41.02	1:1
	F37P20	204.6	0.358	53.82	1.17:1
	G37P25	203.7	0.358	54.57	1.34:1

2.3 Turbulence model

Three major numerical analysis techniques can be used for turbulent flow fields: direct numerical simulation (DNS), large eddy simulation (LES), and Reynolds-averaged Navier-Stokes (RANS) simulation. RANS uses time-based, ensemble-averaged Navier-Stokes equations and models all of the effects from turbulence. Although RANS yields a lower resolution of analysis than DNS or LES, it is widely used in engineering applications due to the practical aspect of not requiring high-resolution calculation grids. The turbulence models for the RANS equations are for computing the Reynolds stresses tensor from the turbulent fluctuations in the fluid momentum. The turbulence models such as k-ε, k-ω and SST have become industry standard models and are commonly used for most types of engineering problems. The SST model solves the above problems for switching to the k-ε model in the free-stream and the k-ω model in the viscous sublayer [5]. Sensitivity studies of turbulence models such as Reynolds Stress Model (RSM), k-ε, k-ω and SST were performed on a 127-pin fuel assembly [6]. In that study, the friction factors with the SST model are 1.5− 4.5% higher than that with the k-ε model. The friction factor with the SST model is 1.4− 1.5% smaller than that with the k-w model. Because the SST model switches to the k-ε model and the k-ω model, the value of the friction factor with the SST model is between that with the k-ε model and that with the k-ω model. The minimum grid scale on the fuel rod surface was 5.0×10E−7 mm to capture the laminar to turbulent flow transition with the SST turbulence model the friction velocity y+ is approximately close to 2.5. In this study, the SST model of CFD was used for investigation.

3. Results

3.1 ORNL 19 pin

Fig 2. shows the location of the thermocouple and Power skew region at bundle outlet of ORNL 19 pin.

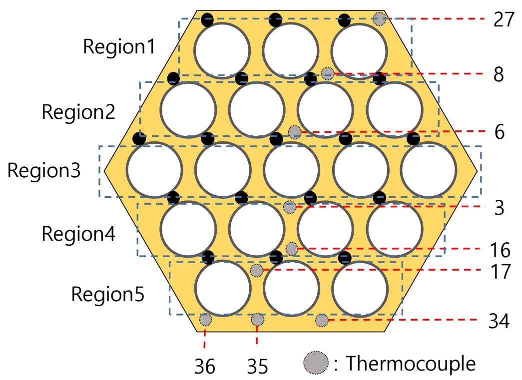

Fig 2. ORNL 19 pin Thermocouples location and Power skew region at bundle outlet

Fig. 2. show the temperature distribution of ORNL 19 pin experimental case Test 2, Test 3 and Test 14. And Fig 3. Show the comparison of experimental and CFD results. In the case of ORNL 19 pin, comparison of normalized outlet temperature was performed for 3 experimental cases (Test 2, Test 3, Test 14). In the case of Test 2, the average relative error is 5.1%, and the maximum error is 10.8%. In the case of Test 3, the average relative error is 4.43%, and the maximum error is 8.5%. In the case of Test 14, the average relative error is 7.65%, and the maximum error is 24.5%.

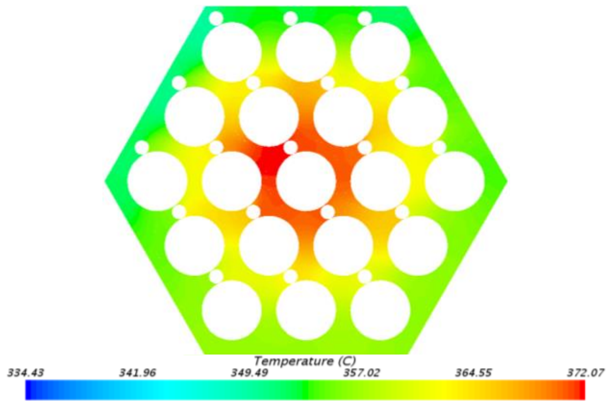

(a) ONRL 19 pin Test 2 (1:1 Skew)

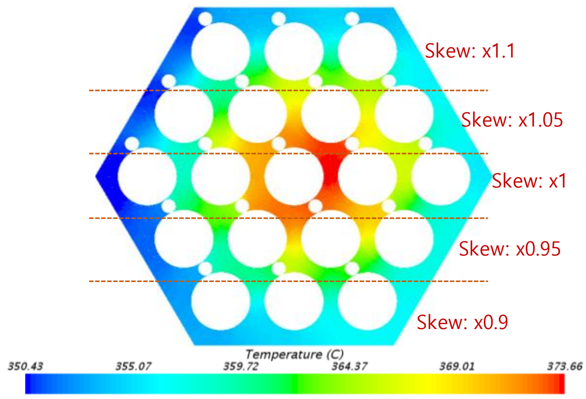

(b) ORNL 19 pin Test 3 (1.2:1Skew)

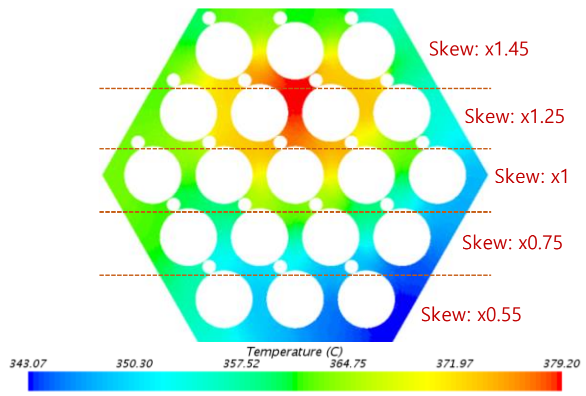

(c) ORNL 19 pin Test 14 (3:1 Skew)

Fig 2. ORNL 19 pin Temperature contour

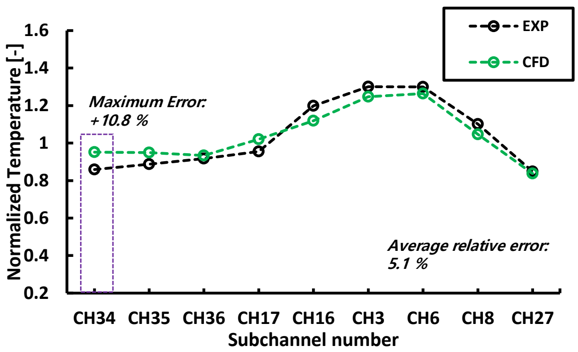

(a) Test 2

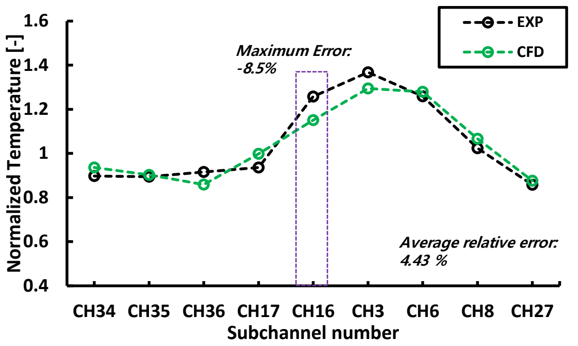

(b) Test 3

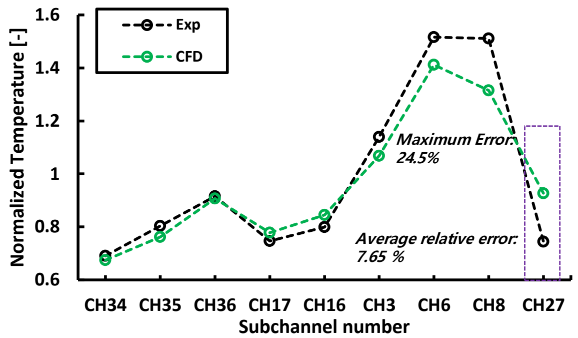

(c) Test 14

Fig 3. Comparison of experimental and CFD result at ORNL 19 pin.

3.2 Toshiba 37 pin

Fig 4. shows the location of the thermocouple and Power skew region at top of heated section of Toshiba 37 pin.

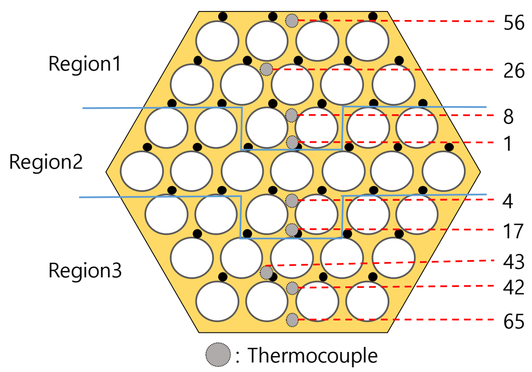

Fig 4. Toshiba 37 pin Thermocouples location and Power skew region at top of heated section

Fig. 5. show the temperature distribution of Toshiba 37 pin experimental case C37P06, F37P20 and G37P25. And Fig. 6. show the comparison of experimental and CFD results. In the case of Toshiba 37 pin, comparison of normalized temperature for the top of heated section was performed for 3 experimental cases (C37P06, F37P20, G37P25). In case of C37P06, the average relative error is 1.66%, and the maximum error is 3.5%. In the case of F37P20, the average relative error is 1.47%, and the maximum error is 3.7%. In the case of G37P25, the average relative error is 4.8%, and the maximum error is 12.4%.

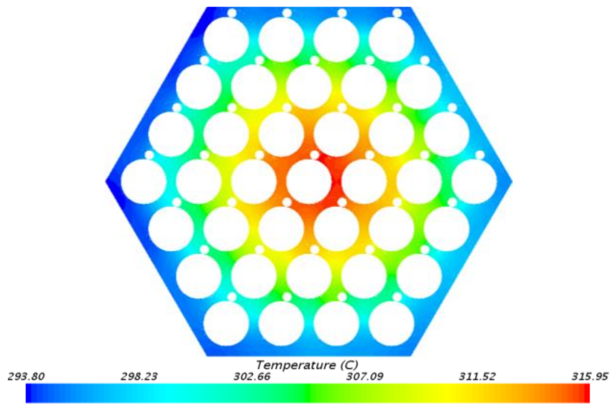

(a) Toshiba 37 pin C37P06 (1:1 Skew)

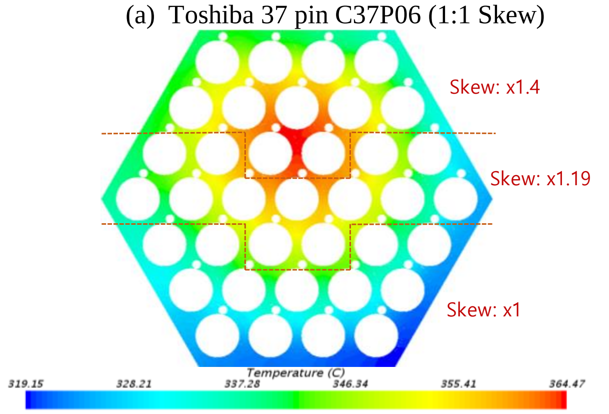

(b) Toshiba 37 pin F37P20

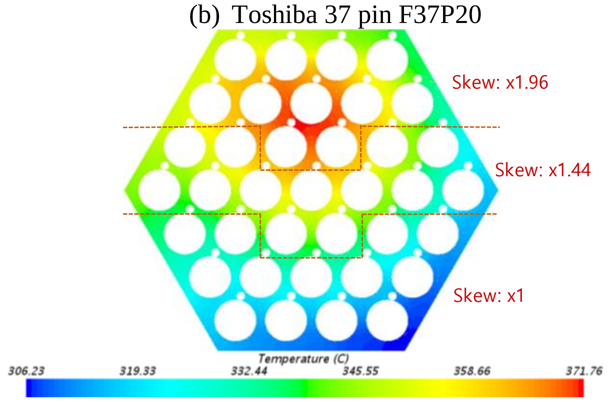

(c) Toshiba 37 pin G37P25

Fig 5. Toshiba 37 pin Temperature contour

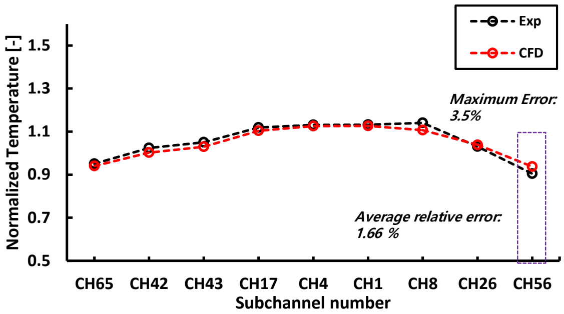

(a) C37P06

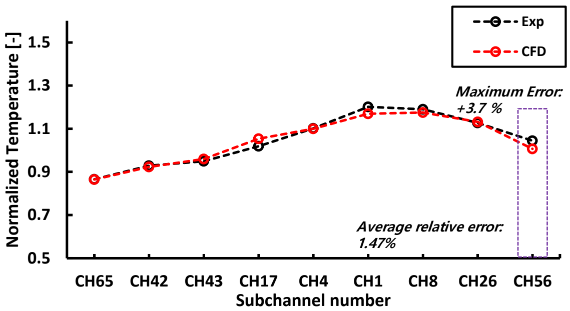

(b) F37P20

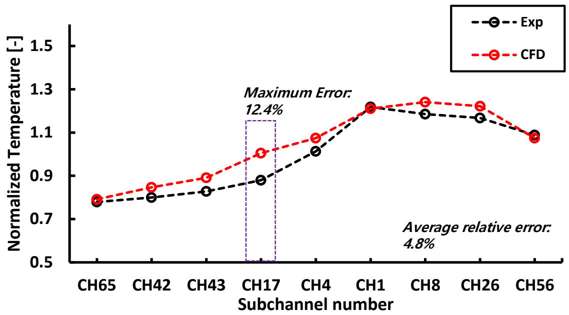

(c) G37P25

Fig 6. Comparison of experimental and CFD result at Toshiba 37 pin.

4. Conclusions

In this study, the numerical investigation was performed by applying the RANS-based CFD methodology to STAR-CCM+ for ONRL 19 pin and Toshiba 37 pin experimental thermal data. In the case of a small radial power skew, the temperature distributions of the experimental results and CFD results were well matched. On the other hand, in the case of a large radial power skew, the temperature distribution tendency was similar, but a relatively large error occurred. In this study, ORNL 19 pin at the outlet and Toshiba 37 pin at the top of heated section was only investigated. Therefore, in the future, we plan to analyze the cause of the error in more detail by comparing and analyzing the experimental results and the CFD results according to the shaft height.

ACKNOWLEDGMENTS

This work was supported by the National Research Foundation of Korea(NRF) grant funded by the Korea government(MSIT) (No. 2021M2E2A2081062), And also supported by Korea Institute of Energy Technology Evaluation and Planning(KETEP) grant funded by the Korea government(MOTIE) (20223030020070).

REFERENCES

[1] M. H. FONTANA, R. E. MacPHERSON, P. A. GNADT, and L. F. PARSLY, “Temperature Distribution in the Duct Wall and at the Exit of a 19-Rod Simulated LMFBR Fuel Assembly (FFM Bundle 2A),” Nucl. Technol., 24, 2, 176-200, (1974).
[2] Namekawa F, Luangdilok W, et al., “Buoyancy and radial power skew effects on wire-wrapped rod bundle thermal hydraulics in an LMFBR fuel assembly”. Proceedings of the Third International Topical Meeting on Reactor Thermal Hydraulics, Vol. 2 16.J-1; 1985.
[3] Yamamoto, K., “An Elliptic-hyperbolic Grid Generation Method and Application to Compressor Flows.”, Special Publication of National Aerospace laboratory, SP 19, pp. 193-198, 1992.
[4] Jae-Ho Jeong, Min-Seop Song, Kwi-Lim Lee, “RANS based CFD methodology for a real scale 217-pin wire-wrapped fuel assembly of KAERI PGSFR”, Nuclear Engineering and Design, vol. 313, pp,.470-485, 2017.
[5] Menter, F.R. “Two-equation eddy-viscosity turbulence models for engineering applications.”, AIAA J. vol. 32 (8), pp. 1598–1605, 1994.
[6] Jae-Ho Jeong, Min-Seop Song, Kwi-Lim Lee, “CFD investigation of three-dimensional flow phenomena in a JAEA 127-pin wire-wrapped fuel assembly”, Nuclear Engineering and Design, vol. 323, pp.166-184, 2017.